

FAST TRACK COMMUNICATION

Time-delay matrix analysis of several overlapping resonances: applications to the helium atom and the positronium negative ion

Keisuke Aiba¹, Akinori Igarashi¹ and Isao Shimamura²¹ Department of Applied Physics, University of Miyazaki, Miyazaki 889-2192, Japan² RIKEN (The Institute of Physical and Chemical Research), Wako, Saitama 351-0198, Japan

Received 27 November 2006

Published 3 January 2007

Online at stacks.iop.org/JPhysB/40/F9**Abstract**

A useful method of analysing sets of several overlapping multichannel resonances, which are extremely difficult to analyse by other means, is presented. It exploits the Lorentzian profiles of eigenvalues $\{q_i(E)\}$ of the energy-dependent time-delay matrix, avoided at their crossings. The contribution to $\{q_i(E)\}$ from each S -matrix pole stands out clearly and uniquely from the contributions from the other poles. Thus the resonances that can be easily missed by the conventional technique of studying the eigenphase sum $\delta(E)$ or its derivative $d\delta/dE$ are singled out as *adiabatic resonances* in a visually unambiguous way. The method is illustrated with the $^1P^o$ continuum states of the helium atom and the positronium negative ion Ps^- below the threshold for $He^+(n=5)$ or $Ps(n=5)$. Many new resonances are found for Ps^- .

(Some figures in this article are in colour only in the electronic version)

Resonance structures often occur in the cross sections for scattering and photoionization. These structures take various shapes due to the formation of quasi-bound states and their interactions with the background continuum. The energy E_r and the width Γ of each quasi-bound state may be calculated by using, for example, the complex-coordinate rotation method [1, 2] as the position $E_r - \frac{1}{2}i\Gamma$ of an S -matrix pole on the complex-energy plane. This method fails to predict how the S -matrix poles affect the resonance shape and the absolute cross section, or even the visibility of the structure.

If the cross section $\sigma(E)$ is known accurately at fine energy mesh points E , then it may be analysed to extract parameters E_r and Γ as well as the parameter representing the resonance shape [3]. However, many resonances are invisible as clear cross section structures. Even the same quasi-bound state can strongly affect the photoionization of ground-state atoms but very weakly that of excited-state atoms, or vice versa [4]. The eigenphase sum $\delta(E)$ for the multichannel continuum wavefunction has long been known to be much more convenient for

resonance analysis. For photoionization, this continuum is the final state and the resonance analysis of $\delta(E)$ is independent of the initial bound state of the process. Regardless of whether the cross section is strongly influenced or not, resonances appear usually as an abrupt increase in $\delta(E)$ in a narrow energy region [5], satisfying the Breit–Wigner one-level formula [6] with the same form as that for the phase shift for single-channel scattering. It has been even more useful and customary to detect sudden changes in the derivative $d\delta(E)/dE$ not only in the electron scattering analysis [7] but also in the photoionization/photodetachment analysis [4, 8].

Another perspective of resonances may be gained from the lifetime matrix or time-delay matrix $Q(E)$, defined by Smith [9] as a generalization of the time delay in single-channel scattering [10, 11]. Smith proved its relation to the S matrix,

$$Q(E) = i\hbar S \frac{dS^\dagger}{dE} = -i\hbar \frac{dS}{dE} S^\dagger = Q^\dagger(E), \quad (1)$$

where the dagger indicates the Hermitian conjugate. This relation is often referred to as defining the Q matrix. For single-channel scattering, $S = \exp(2i\delta)$ with a partial-wave phase shift δ . Then, equation (1) shows that $Q = 2\hbar d\delta/dE$. This is the additional time spent by the projectile in scattering compared with a passage in the absence of any interactions with the target, hence ‘time delay’ [10, 11]. For multichannel scattering the diagonal elements Q_{ii} are real and have the meaning of the time delay averaged over all possible final channels, starting from initial channel i . A matrix analysis proves that the trace, or the diagonal sum, of the Q matrix is related to the eigenphase sum by

$$2\hbar \frac{d\delta}{dE} = \text{Tr } Q(E) \equiv \sum_i Q_{ii}(E) = \sum_i q_i(E) \quad (2)$$

for $S(E)$ or $\delta(E)$ of any E -dependence, either in the presence or absence of resonances, either isolated or overlapping [12]. Here, $\{q_i\}$ are the eigenvalues of the Q matrix. The Breit–Wigner formula for $\delta(E)$ used in (2) immediately leads to a Lorentzian profile of $\text{Tr } Q(E)$ lying on top of a slowly varying background time delay. When a resonance occurs, not only $\text{Tr } Q(E)$ but also the largest eigenvalue carries the Lorentzian profile [9] and has been studied in some detail in the literature [13–15].

Furthermore, detailed investigation of all the eigenvalues $\{q_i(E)\}$ as well as $\text{Tr } Q(E)$ elucidates intriguing resonance dynamics [12, 16]. In some cases in positron scattering by the helium ion, $e^+ + \text{He}^+$, and electron or positron scattering by the positronium, $e^\pm + \text{Ps}$, the largest eigenvalue shows a typical Lorentzian profile, whereas $\delta(E)$ decreases monotonically, indicating average time advance instead of time delay [12, 16]. This arises from the logarithmic divergence of the background eigenphase sum towards the threshold of the formation of $\text{Ps}(n)$ in an excited state n . The complex rotation method cannot assess these significant interactions of an S -matrix pole with the strong background continuum that mask the effects of a pole on the scattering cross section.

When two or more resonances overlap each other, the analysis of $\sigma(E)$ or the S matrix is extremely complicated. However, an illuminating phenomenon occurs in the eigenvalues $\{q_i(E)\}$ and their sum, $\text{Tr } Q(E)$. The eigenphase sum $\delta(E)$ and $\text{Tr } Q$ take simple forms involving the background eigenphase sum $\delta_b(E)$,

$$\delta(E) = \sum_{\nu=1}^N \arctan \frac{\Gamma_\nu/2}{E_\nu - E} + \delta_b(E), \quad (3)$$

$$\text{Tr } Q(E) = \sum_{\nu=1}^N L_\nu(E) + 2\hbar \frac{d\delta_b(E)}{dE} \equiv \sum_{\nu=1}^N \frac{\hbar\Gamma_\nu}{(E - E_\nu)^2 + (\Gamma_\nu/2)^2} + 2\hbar \frac{d\delta_b(E)}{dE}, \quad (4)$$

for N overlapping resonances at E_ν and with widths Γ_ν [17]. These are of the same forms as the well-known overlapping resonance formulae for single-channel problems. In particular, $\text{Tr } Q(E)$ is a mere superposition of Lorentzian curves $L_\nu(E)$ except for the usually small background. For double resonances, it has been proved analytically that two eigenvalues $\{q_i(E)\}$ take such Lorentzian profiles avoided from each other only near their crossing point, either strongly or weakly, depending on the strength of the interaction between the two resonances [17]. The eigenvalue curves look almost like crossing Lorentzians if the interaction is weak, but careful examination is necessary for recognizing the avoided crossing behaviour if the interaction is strong.

In the present work, we examine the Q -matrix eigenvalues $\{q_i(E)\}$ for He and the negative ion Ps^- numerically in detail. In particular, cases of *several* overlapping resonances, which are extremely difficult to analyse by any conventional method, will be treated with remarkable results proving the power of the Q -matrix-eigenvalue technique. All numerical values in this paper are given in atomic units.

Just as in our previous work [4, 8, 12, 16–19], we use the hyperspherical close-coupling (HSCC) method, described in some detail in [18, 19]. Briefly, the six-dimensional hyperspherical coordinate system for the three particles consists of the reaction coordinate called the hyperradius ρ and the five angular coordinates, denoted collectively by Ω . The hyperradius for He is defined by $\rho^2 = r_1^2 + r_2^2$ in terms of the radial distances r_i ($i = 1, 2$) of the electrons from the He nucleus. For Ps^- , ρ is defined by $\rho^2 = \frac{2}{3}R_j^2 + \frac{1}{2}r_j^2$ using either of the two sets of Jacobi coordinates $(\mathbf{r}_j, \mathbf{R}_j)$ ($j = 1, 2$), where \mathbf{r}_j is the position vector of the j th electron e_j^- from the positron e^+ , and \mathbf{R}_j the relative-distance vector from the centre of mass of the $e_j^-e^+$ pair to the other electron. The two sets of Jacobi coordinates are shown to define a common ρ . All the asymptotic channels, $e^- + \text{He}^+$ and $e^- + \text{Ps}$, are represented by large values of ρ .

The Hamiltonian consists of the term $h_{\text{ad}}(\Omega; \rho)$ adiabatic in ρ and the nonadiabatic operators in ρ . The eigenfunctions of $h_{\text{ad}}(\Omega; \rho)$ define adiabatic hyperspherical states, the corresponding eigenvalues $\{U_i(\rho)\}$ being adiabatic hyperspherical potentials similar to the adiabatic molecular potentials. The potential curves $\{U_i(\rho)\}$ are useful for elucidating the dominant dynamics of the three-body system. Bound states supported by the lowest potential of particular symmetry are approximations to three-body bound states. Bound states supported by an excited potential turn into Feshbach resonances due to the nonadiabatic coupling. Shape resonances formed inside a potential barrier usually remain as shape resonances even with the nonadiabatic coupling taken into account. Thus, bound states and resonances may be visually analysed by the inspection of the adiabatic hyperspherical potentials $\{U_i(\rho)\}$.

For accurate calculations of $\text{He}(^1\text{P}^0)$ and $\text{Ps}^-(^1\text{P}^0)$ we take account of the nonadiabatic operators and solve coupled equations, or the HSCC equations, up to a large value of ρ , where the hyperspherical channels are connected to the physical channels defined in terms of the Jacobi coordinates. The reactance and scattering matrices are obtained from their asymptotic forms, which involve the dipole states explicitly [20], so that the often crucial effects of the long-range dipole potentials are automatically taken into account up to infinitely large distances. All channels dissociating asymptotically into $e^- + \text{He}^+$ ($n = 1-6$) and $e^- + \text{Ps}$ ($n = 1-6$) are coupled in this work.

Figure 1(a) shows adiabatic hyperspherical potentials of $\text{He}(^1\text{P}^0)$ converging asymptotically to the energy E_n of $\text{He}^+(n)$ ($n = 4, 5, 6$). Since all these potentials have an asymptotic form $-2n^{-2} - \rho^{-1}$, any of them, whether deep or shallow, supports an infinite Rydberg series of Feshbach resonances due to the attractive Coulomb tail. A few curves converging to E_6 have a minimum below E_5 and above -0.10 . Thus, the lower members (having the total energy E in the range $-0.10 < E < -0.08$) of Rydberg series supported

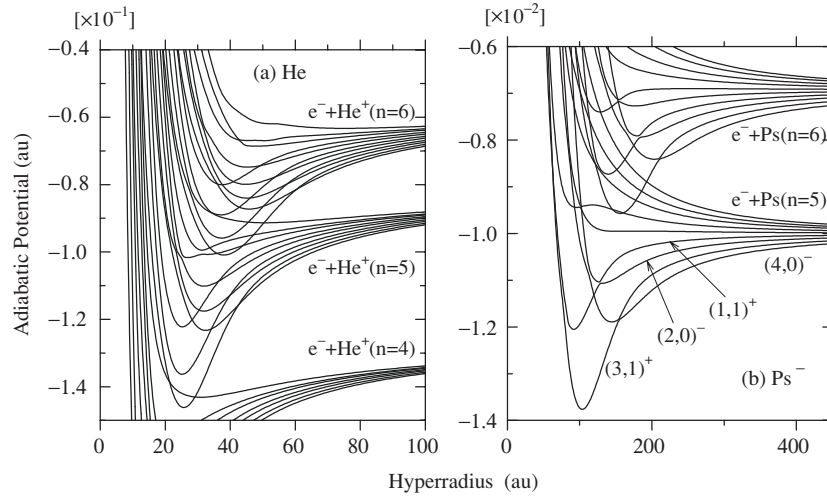


Figure 1. Adiabatic hyperspherical potential curves. (a) He($^1P^0$). (b) Ps($^1P^0$); the potentials supporting an infinite series of Feshbach resonances below the energy of Ps ($n = 5$) are labelled in terms of the correlation quantum numbers (K, T)^A.

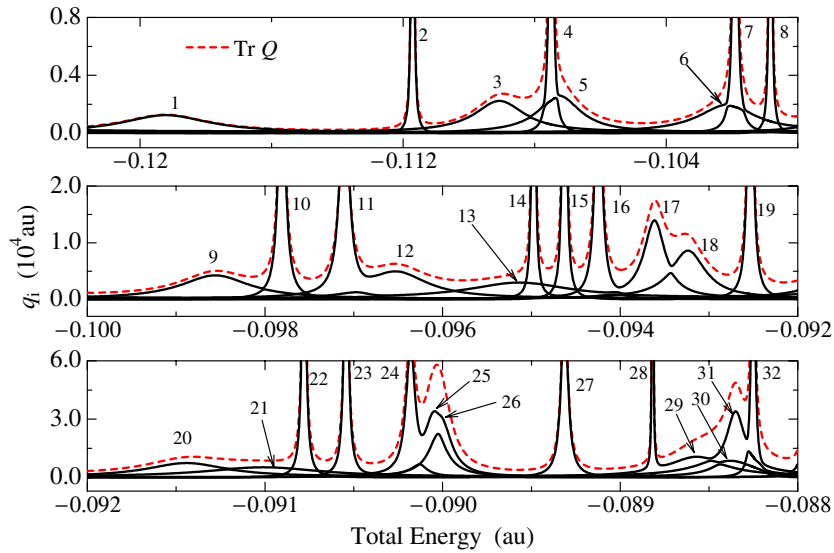


Figure 2. The eigenvalues $\{q_i(E)\}$ of the time-delay matrix $Q(E)$ for He($^1P^0$) and their sum, $\text{Tr } Q(E)$, plotted against the total energy E .

by these curves may well act as intruders into the Rydberg series converging to E_5 , resulting in overlapping resonances. Members (lying either below or above $E = -0.10$) of different Rydberg series converging to E_5 may also overlap.

All the sixteen eigenvalues $\{q_i(E)\}$ of the Q matrix and their sum, $\text{Tr } Q(E)$, are plotted in figure 2 for $-0.121 < E < -0.088$, i.e. below E_5 , although many $\{q_i(E)\}$ are too small to distinguish from the base line. Partial photoionization cross sections and the photoelectron

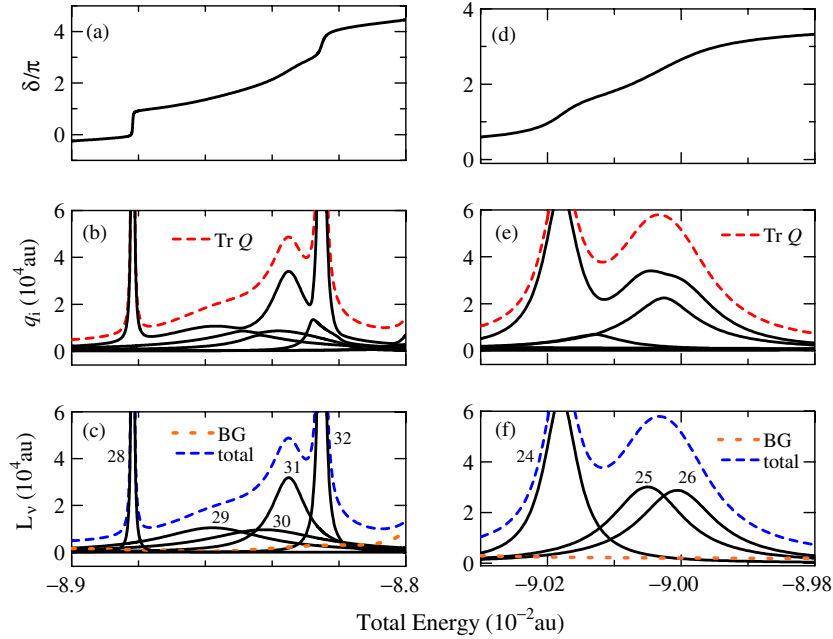


Figure 3. Left: the energy region of the He($1P^0$) overlapping resonances 28–32. Right: That of resonances 24–26. (a) and (d) Eigenphase sum $\delta(E)$. (b) and (e) The eigenvalues $\{q_i(E)\}$ of the Q matrix and their sum, $\text{Tr } Q(E) (= 2\hbar d\delta/dE)$. (c) and (f) The Lorentzians $L_v(E)$ representing the diabatic resonances, the background (BG) and their sum, obtained by fitting $\text{Tr } Q$ to equation (4).

angular distributions of He in this energy region were previously measured in detail and analysed by HSCC calculations [21]. Attention was paid to a doubly overlapping resonance arising from the interference between a Rydberg series converging to E_5 and an intruder from an $n = 6$ series; no time-delay analysis was tried in that work. The Q -matrix trace in figure 2 is seen to take a form (4) of the superposition of Lorentzian peaks $L_v(E)$. These resonances are supported by the hyperspherical potentials shown in figure 1(a). Some peaks in figure 2 (labelled 1, 2 and 27) are fairly well isolated from any other peak. However, many others present typical cases of overlapping resonances. Breaking down the trace into the eigenvalues, we gain a much better understanding of how the originally different resonances are superimposed into a set of overlapping resonances. Some eigenvalues $\{q_i(E)\}$ have Lorentzian profiles, avoided from each other only near the crossing points of the Lorentzians. In fact, most avoided crossings found in figure 2 appear as if they were real crossings. Further detail may be elucidated by magnifying some parts of figure 2, as is done in figure 3.

Rapid increase in the eigenphase sum $\delta(E)$ is noticeable at two places in figure 3(a), suggesting two resonances occurring there. Another resonance emerges in $\text{Tr } Q(E)$ in figure 3(b), showing that the derivative $d\delta/dE$ is a better probe of resonances than $\delta(E)$ itself. An even more sensitive probe turns out to be the eigenvalues $\{q_i(E)\}$ in figure 3(b). Quite obvious avoided crossings with weak avoidance or weak resonance interaction are observed, which, if diabatically connected, reveal as many as five Lorentzian peaks in this energy region. At least two of them (resonances 29 and 30) would have been missed by the conventional techniques of analysing scattering calculations. The detailed resonance structure in $\{q_i(E)\}$ having been uncovered, equation (4) with five Lorentzians and a background of polynomial

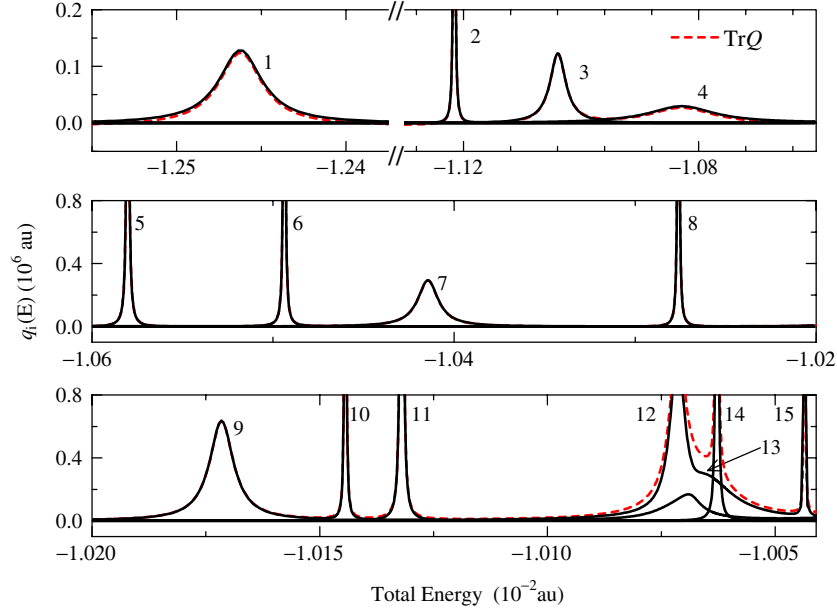


Figure 4. The eigenvalues $\{q_i(E)\}$ of the time-delay matrix $Q(E)$ for $\text{Ps}^-(^1\text{P}^0)$ and their sum, $\text{Tr } Q(E)$, plotted against the total energy E .

in E of a low degree is now fitted to the calculated $\text{Tr } Q(E)$ of figure 3(b). This fitting is extremely accurate with no appreciable deviation of the fitted curve (blue broken curve in figure 3(c)) from the calculated $\text{Tr } Q(E)$ (red broken curve in figure 3(b)) if drawn in the same figure. Figure 3(c) includes all the five obtained Lorentzian profiles, which are effectively the diabaticization of $\{q_i(E)\}$ and may be called *diabatic resonances*. This diabaticization affords a transparent visual understanding of the overlapping resonances. Figure 3(c) also displays the small background, which starts to rise towards the right end of the figure due to the tail of an adjacent resonance not taken into account explicitly in the present analysis.

Another case quite different from the above is found in the range $-0.0903 < E < -0.0898$. The eigenphase sum $\delta(E)$ in figure 3(d) increases nearly by 3π in this energy range, suggesting the possibility of three resonances. However, an appreciable slope change in $\delta(E)$ occurs only twice, which is indeed supported by $\text{Tr } Q(E)$ in figure 3(e) having only two peaks. In fact, the largest Q -matrix eigenvalue in figure 3(e) has a weak kink just below $E = -9.00 \times 10^{-2}$, which, together with the broad peak in the next largest eigenvalue in the same energy range, represents quite a strongly avoided crossing between two resonances. Including another marked peak at lower energies, we detect three resonances. Thus, a three-Lorentzian fit of $\text{Tr } Q(E)$ is appropriate. This leads to figure 3(f) of diabatic resonances similar to figure 3(c). Indeed, the strong interactions between resonances 25 and 26 are seen to generate the avoided crossing in $\{q_i(E)\}$ of figure 3(e) around $E = -9.00 \times 10^{-2}$, and the two avoided crossings between resonance 24 and the strongly interacting resonances 25/26 are not separated well.

Figure 1(b) shows adiabatic hyperspherical potentials of $\text{Ps}^-(^1\text{P}^0)$ breaking up into $e^- + \text{Ps}$ ($n = 5, 6$). Due to the degenerate sublevels of Ps ($n \geq 2$), the asymptotic potentials $E_n + \frac{1}{2}\alpha\rho^{-2}$ ($E_n = -\frac{1}{4}n^{-2}$) have a dipole term with a channel-dependent constant α . If

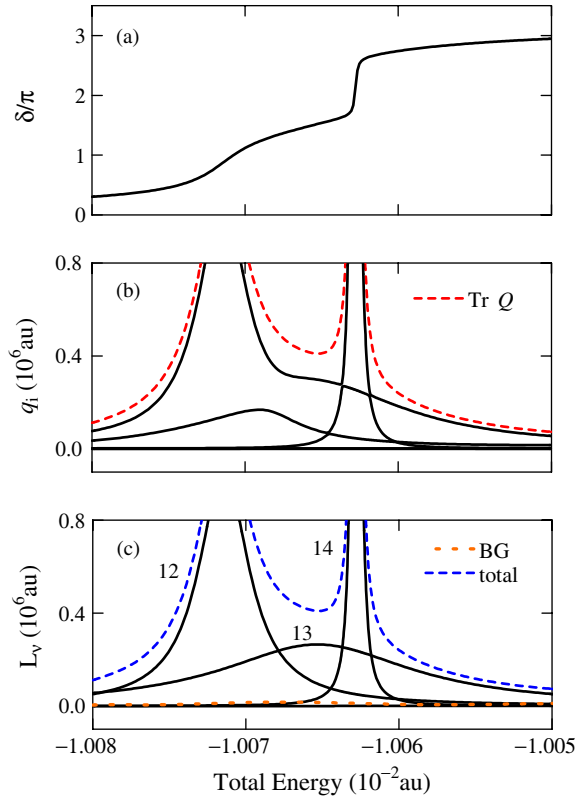


Figure 5. The energy region of the $\text{Ps}^- (^1\text{P}^0)$ overlapping resonances 12–14. (a) Eigenphase sum $\delta(E)$. (b) The eigenvalues $\{q_i(E)\}$ of the Q matrix and their sum, $\text{Tr } Q(E) (= 2\hbar d\delta/dE)$. (c) The three Lorentzians $L_\nu(E)$ representing the diabatic resonances, the background (BG) and their sum.

$\alpha < -\frac{1}{4}$, an infinite series of Feshbach resonances is supported [20]. Only four of the potentials converging to $E_5 (= -0.01)$, labelled in figure 1(b) using the correlation quantum numbers $(K, T)^A$ [22, 23], satisfy this condition. The others lie above E_5 at all values of ρ . Because of this, and also because all the potentials converging to E_6 lie higher than E_5 , not too many overlapping resonances are expected below E_5 .

Figure 4 displays $\{q_i(E)\}$ and their sum, $\text{Tr } Q(E)$, below E_5 . Just as in figure 2 for He, many $\{q_i(E)\}$ are too small to distinguish from the base line. Most peaks in $\text{Tr } Q$ are well isolated from any other peak as expected, and are almost indistinguishable from the largest eigenvalue. Thus, the conventional resonance analysis techniques are already good enough for them. A set of overlapping resonances appears in the energy range $-1.008 \times 10^{-2} < E < -1.005 \times 10^{-2}$, which is studied in detail in figure 5. The eigenphase sum $\delta(E)$ in figure 5(a) increases by about 3π in this energy range, suggesting three resonances. However, an appreciable slope change in $\delta(E)$ occurs only twice and $\text{Tr } Q(E)$ in figure 5(b) shows only two peaks. Again breaking down $\text{Tr } Q(E)$ into $\{q_i(E)\}$ as in figure 5(b), one finds a strongly avoided crossing between the two largest Q -eigenvalues in between the two peaks in $\text{Tr } Q(E)$. It discloses a third, broad resonance (number 13). It is most probably missed in the usual procedure of analysing scattering calculations, but is clearly seen in figure 5(c) for the diabatic resonances.

Table 1. The energies E_r and widths Γ (in au) of $^1P^0$ resonances in Ps^- lying below the threshold $E_5 = -1.0000 \times 10^{-2}$ au of Ps ($n = 5$). $x[y] = x \times 10^y$.

Resonance number	Classification (K, T) ^A	Present HSCC		Complex rotation [25]	
		E_r	Γ	E_r	Γ
1	(3, 1) ⁺	-1.2462 [-2]	3.07 [-5]	-1.2463 [-2]	3.05 ± 0.1 [-5]
2	(4, 0) ⁻	-1.1215 [-2]	1.94 [-6]	-1.1216 [-2]	2.7 [-6]
3	(3, 1) ⁺	-1.1039 [-2]	3.22 [-5]	-1.1044 [-2]	3.15 ± 0.1 [-5]
4	(1, 1) ⁺	-1.0829 [-2]	1.34 [-4]	-1.0830 [-2]	1.36 ± 0.01 [-4]
5	(4, 0) ⁻	-1.0580 [-2]	1.31 [-6]		
6	(2, 0) ⁻	-1.0493 [-2]	8.81 [-7]		
7	(3, 1) ⁺	-1.0414 [-2]	1.36 [-5]		
8	(4, 0) ⁻	-1.0276 [-2]	7.42 [-7]		
9	(3, 1) ⁺	-1.0171 [-2]	6.34 [-6]		
10	(2, 0) ⁻	-1.0144 [-2]	1.22 [-7]		
11	(4, 0) ⁻	-1.0132 [-2]	3.67 [-7]		
12	(3, 1) ⁺	-1.0071 [-2]	3.95 [-6]		
13	(1, 1) ⁺	-1.0065 [-2]	1.51 [-5]		
14	(4, 0) ⁻	-1.0062 [-2]	2.11 [-7]		
15	(2, 0) ⁻	-1.0043 [-2]	4.53 [-8]		

We have detected many resonances in $\text{Ps}^- (^1P^0)$ that we found in no literature. The calculated resonance parameters are given in table 1, where the assignment follows the procedure in [24]. The four lowest resonances were found previously in complex rotation calculations [25]; good agreement with the present results is seen.

The S matrix and the cross section for a multichannel continuum process get extremely complicated when more than two resonances overlap each other. The conventional method of analysing calculated continuum processes to extract resonance information has been to fit the eigenphase sum $\delta(E)$ or its derivative $d\delta/dE$ to the Breit–Wigner multi-level formula. The present work reveals that this method can easily miss some resonances. This has been illustrated on $\text{He} (^1P^0)$ and $\text{Ps}^- (^1P^0)$ below the threshold for $\text{He}^+ (n = 5)$ or $\text{Ps} (n = 5)$ by careful examination of the avoided crossings of the eigenvalues of the time-delay matrix $Q(E)$, followed by diabaticization of the overlapping resonances. Each *diabatic resonance*, including any that is invisible in $\delta(E)$ or $d\delta/dE$, stands remarkably clearly as a Lorentzian out of the other resonances in the figure of the Q -matrix eigenvalues. The resonance analysis technique presented in this work must be powerful in the broad area of atomic, molecular and nuclear physics.

Acknowledgment

This work was supported in part by the grant-in-aid for Scientific Research from Japan Society for the Promotion of Science.

References

- [1] Ho Y K 1983 *Phys. Rep.* **99** 1
- [2] Moiseyev N 1998 *Phys. Rep.* **302** 211
- [3] Fano U 1961 *Phys. Rev.* **124** 1866
- [4] Tang J-Z and Shimamura I 1994 *Phys. Rev. A* **50** 1321

- [5] Hazi A U 1979 *Phys. Rev. A* **19** 920
- [6] Blatt J M and Weisskopf V F 1979 *Theoretical Nuclear Physics* (New York: Springer) chapter X
- [7] Tennyson J and Noble C J 1984 *Comput. Phys. Commun.* **33** 421
- [8] Igarashi A and Shimamura I 1997 *Phys. Rev. A* **56** 4733
- [9] Smith F T 1960 *Phys. Rev.* **118** 349
- [10] Bohm D 1951 *Quantum Mechanics* (New York: Prentice-Hall) chapter 11
- [11] Wigner E P 1955 *Phys. Rev.* **98** 145
- [12] Igarashi A and Shimamura I 2004 *Phys. Rev. A* **70** 012706
- [13] Burke P G, Cooper J W and Ormonde S 1969 *Phys. Rev.* **183** 245
- [14] Sadeghpour H R, Greene C H and Cavagnero M 1992 *Phys. Rev. A* **45** 1587
- [15] Stibbe D T and Tennyson J 1996 *J. Phys. B: At. Mol. Opt. Phys.* **29** 4267
- [16] Igarashi A and Shimamura I 2004 *J. Phys. B: At. Mol. Opt. Phys.* **37** 4221
- [17] Shimamura I, McCann J F and Igarashi A 2006 *J. Phys. B: At. Mol. Opt. Phys.* **39** 1847
- [18] Igarashi A, Toshima N and Shirai T 1994 *Phys. Rev. A* **50** 4951
- [19] Igarashi A, Shimamura I and Toshima N 2000 *New J. Phys.* **2** 17
- [20] Gailitis M and Damburg R 1963 *Proc. Phys. Soc. London* **82** 192
- [21] Menzel A, Frigo S P, Whitfield S B, Caldwell C D, Krause M O, Tang J-Z and Shimamura I 1995 *Phys. Rev. Lett.* **75** 1479
- [22] Herrick D R 1975 *Phys. Rev. A* **12** 413
- [23] Lin C D 1986 *Adv. At. Mol. Phys.* **22** 77
- [24] Ho Y K and Greene C H 1986 *Phys. Rev. A* **35** 3169
- [25] Ho Y K and Bhatia A K 1991 *Phys. Rev. A* **44** 2890